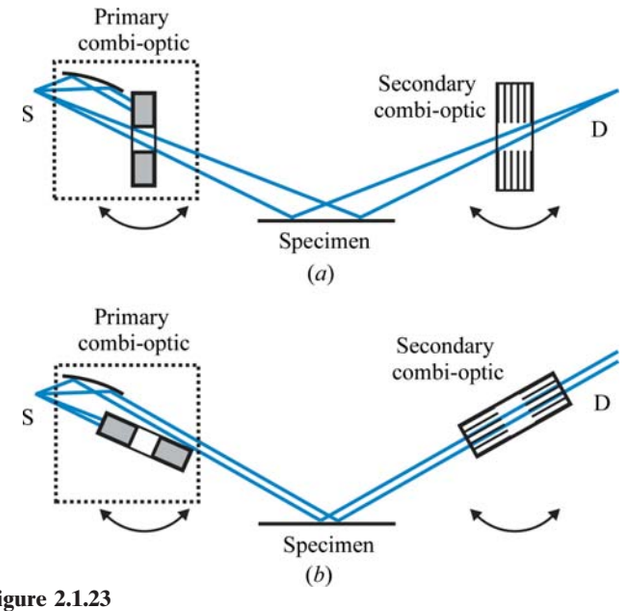

Figure 2.1.23
Incident and diffracted beam combi-optics for switching between (*a*) the Bragg–Brentano geometry and (*b*) the parallel-beam geometry. S: X-ray source; D: detector.

separated by a small gap. When turning the two parallel-plate collimators into the beam direction, only those diffracted rays running parallel to the collimator plates will reach the detector (Fig. 2.1.23*b*). When turning the collimators by approximately 90°, the gap between the two collimators acts as a variable slit enabling a divergent beam (Fig. 2.1.23*a*).

Significantly more sophisticated combi-optics are used in X-ray diffractometers that are mostly used for thin-film analysis. In Fig. 2.1.24 an example for two different incident-beam and four different diffracted-beam paths is shown, providing the choice between eight different beam paths depending on the properties of the specimen and the application requirements. The incident beam path is characterized by a fixed-target X-ray source equipped with a Göbel mirror, attached on a motorized mount. By rotating this arrangement by about 5°, the beam travels either through a rotary absorber followed by a two-bounce channel-cut monochromator and a slit (upper beam path, high-resolution setting), or just through a single slit (lower beam path, high-flux setting). The diffracted beam path represents a double-detector setup, typically consisting of a point detector (D1) and a position-sensitive detector (D2). For the point detector three different beam paths can be chosen by means of a switchable slit, which either sends the beam through a three-bounce channel-cut analyser, or through the same two-parallel-plate-collimator arrangement already discussed in Fig. 2.1.23, either acting as a parallel-plate collimator or a variable slit. A fourth beam path without any diffracted-beam X-ray optics allows use of the position-sensitive detector.

2.1.7. X-ray detectors

The general concepts of X-ray detectors are described here with the focus on practical aspects. The physics of X-ray detection and the individual detector technologies are extensively covered in the literature. He (2009) gives a comprehensive discussion that also includes the most recent detector technologies. Additional detailed descriptions are found in *International Tables for Crystallography* Vol. C (2004), as well as in the textbooks by Pecharsky & Zavalij (2009), Clearfield *et al.* (2008), Paganin (2006), Jenkins & Snyder (1996), and Klug & Alexander (1974).

2.1.7.1. *Detector parameters*

There are many ways to characterize the properties and performance of an X-ray detector.

Ideally, in a given detector operated under appropriate conditions, (1) each photon will produce a detectable signal and (2) the signal recorded is proportional to the number of photons detected. If both conditions are fulfilled then the detector has unit *quantum efficiency*. The *detective quantum efficiency* (DQE) may be defined as the squared ratio of the output signal-to-noise ratio to the input signal-to-noise ratio, expressed as a percentage. A detector's DQE is generally less than 100% because there is always detector noise and not every photon is detected. The DQE thus depends on the characteristics of the detector (*e.g.* transmission of the detector window, count rates and dead time, *etc*.) and varies with the X-ray energy for the same detector.

The *detector linearity* determines the accuracy of intensity measurements and depends on the ratio between the photon

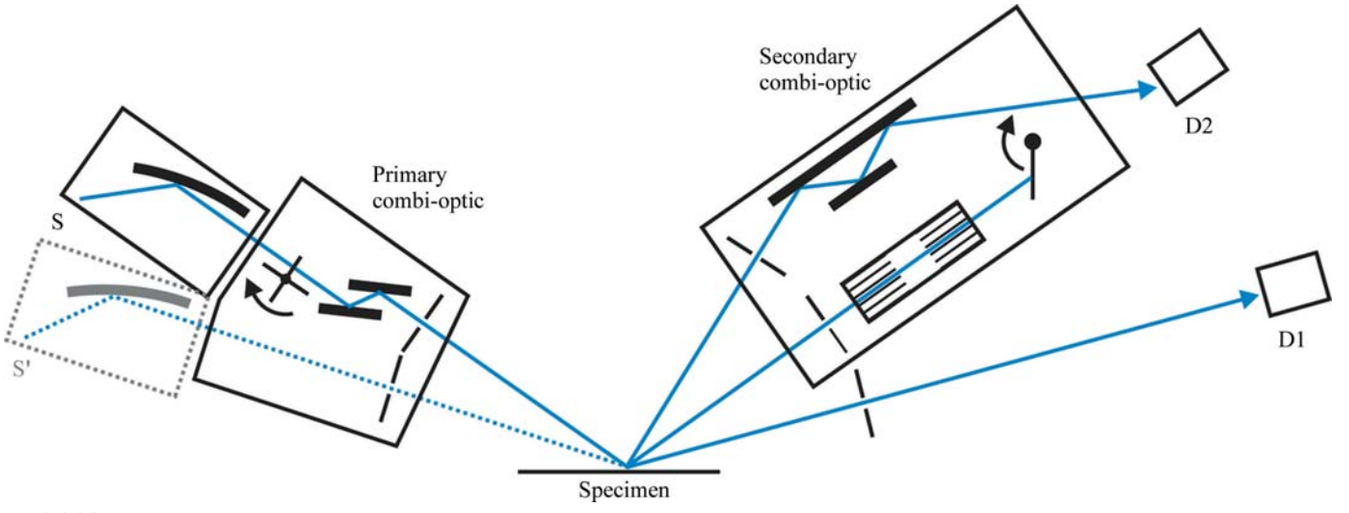

Figure 2.1.24
Example of the use of highly sophisticated incident- and diffracted-beam combi-optics in combination with a rotatable X-ray source and a double detector arm. This setup enables two different incident-beam and four different diffracted-beam paths, and thus provides a choice between eight different beam paths, depending on the properties of the specimen and the requirements of the application. S: X-ray source, S′: X-ray source rotated by about 5°, D1, D2: detectors.

count rate and the rate of signals generated and registered by the detector. In any detector it takes some time to process the conversion of an individual photon to a voltage pulse, which is related to the detector *dead time*: photons arriving while the detector is still processing the previous photon conversion may be lost. The detector dead time is related to the physical characteristics of the detector, *e.g.* the drift time in a gas-ionization detector, or the read-out time of the counting electronics, *e.g.* the shaping time of the amplifier. The effect of dead time becomes a substantial issue at high photon count rates, when the dead time becomes a significant part of the average time separation between two arriving photons, leading to increasing intensity losses at higher count rates. Detectors can be categorized as being non-paralysable or paralysable with respect to dead time. A non-paralysable detector is dead for a fixed time after each count, but not influenced by photons arriving during the dead time. Counting losses increase with increasing count rates, but the true count rate of a nonparalysable detector can be corrected unless the maximum observed count rate is equal to the inverse of the dead time. In a paralysable detector, a second photon arriving within the dead time can not be counted but will extend the dead time up to a point where the detector will be incapable of collecting any counts at all (saturation point). Modern detectors can stand the count rates obtained in powder diffraction experiments using fixed-target X-ray sources. At very high count rates, *e.g.* those obtained in thin-film experiments such as reflectometry, it may be necessary to attenuate the beam. Sophisticated instruments are equipped with an electronic feedback system and automatic absorbers (see Section 2.1.6.3.1.2) to ensure that detector saturation is avoided.

The *dynamic range* of a detector may be defined as the range between the smallest detectable photon count rates (determined by inherent detector noise such as readout and dark noise) to the largest acceptable photon count rates (determined by the dead time).

Energy resolution is the ability of a detector to resolve two photons that have different energies. Energy resolution is typically characterized by the size of the detector energy window, ΔE, in electron volts, as determined by the full width at half maximum (FWHM) of the detector-efficiency curve as a function of energy, with the detector and counting electronics set to a specific wavelength. Another frequently used expression for energy resolution is the ratio of the detector energy window size to the energy of the monochromatic X-ray beam, E, expressed as $\Delta E/E$.

The *proportionality* of the detector determines how the size of the generated voltage pulse is related to the energy of the absorbed X-ray photons, and electronic methods (pulse-height selection) can be used to discriminate between different energies. An accurate proportionality thus allows the use of *energy discrimination* as a form of monochromatization, where the energy is filtered by the detector rather than by an optical element such as a metal filter, crystal or mirror; see Section 2.1.6.3. Signals corresponding to photons with too high or too low energies are discarded.

The size and weight of detectors may impose several practical constraints, see also Section 2.1.4.2. For large detectors the accessible angular range may be limited owing to collision issues. For heavy detectors a horizontal goniometer may be preferred over a vertical goniometer (unless horizontal specimen positioning is imperative) in order to minimize the goniometer load.

X-ray detectors may be broadly classified as *counting detectors* or *integrating detectors*. Counting (digital) detectors are able to detect and count individual photons. The number of pulses counted per unit time is proportional to the incident X-ray flux. Integrating (or analogue) detectors accumulate photon-induced signals for a given period of time, prior to the integrated signal being read out and converted into an (analogue) electrical signal. The signal size is proportional to the flux density of the incident X-rays.

Counting and integrating detectors each have their clear advantages and disadvantages. Counting detectors normally have a greater dynamic range than integrating detectors, while integrating detectors normally have better spatial resolution (Section 2.1.7.3). Energy resolution is only possible for counting detectors. Readout and dark noise are usually higher for integrating detectors. Integrating detectors are not limited by the photon count rate as there is no dead time; nevertheless, the measurement time has to be kept sufficiently small to avoid saturation.

2.1.7.2. *Detector types*

Counting and integrating detectors can be further distinguished by their working principle, and are represented by scintillation, gas-ionization and semiconductor detectors. The most commonly used detector types and their properties are listed in Tables 2.1.1 and 2.1.6, respectively.

At the end of the 1990s the types of detectors in use were scintillation, gas-ionization, Si(Li) and image-plate detectors, with the scintillation counter being the most common by far. Usage of photographic film had already greatly diminished by that time. With the introduction of a series of new one- and two-dimensional detector technologies since the late 1990s, the X-ray detection landscape changed completely. New semiconductor-based detectors (silicon micro-strip, silicon pixel) as well as gas-ionization-based detectors (micro-gap) reached a market share of >90% in newly sold X-ray powder diffractometers within only a few years. As a consequence, classical metal-wire-based proportional counters and scintillation counters will probably become obsolete before 2020. The same is expected for CCD-based detectors, which will be replaced by the very recently introduced complementary metal–oxide–semiconductor (CMOS) active pixel sensor technology.

In the following the working principles of currently available detector types will be briefly described. Matters that are specific to zero- (0D), one- (1D) and two-dimensional (2D) detection are discussed in Section 2.1.7.3. While image plates are still in use, their market share in newly sold systems has become insignificant. Photographic film techniques are totally obsolete. For these reasons, these two detector types will not be taken into further consideration.

2.1.7.2.1. *Scintillation counters*

Scintillation counters are constructed from a scintillator crystal optically coupled to a photomultiplier tube. The crystal is typically made of sodium iodide (NaI) doped with about 1% thallium, frequently denoted as NaI(Tl). When irradiated by X-ray radiation, blue light (∼415 nm) is emitted and converted to electrons in a photomultiplier and amplified; the resulting pulses are registered as photon counts.

The height of the outgoing pulses is proportional to the energy of the incoming X-ray photons. This permits the use of pulse-height selection but only allows for poor energy resolution. The relatively high count rate and a moderate noise level result in a moderate dynamic range. These characteristics are the reason for the formerly wide-ranging acceptance of the scintillation counter

Table 2.1.6
Important detector properties at 8 keV as reported by various vendors

Only typical values are given to allow approximate comparisons. Detector properties strongly depend on individual detector designs and are subject to high development rates.

		Gas ionization (Xe/CO_2 gas filling)		
	Scintillation	Wire based (0D)	Wire based (1D/2D)	Micro-gap (1D/2D)
DQE	∼95%	∼95%	∼80%	∼80%
Dynamic range	$>6 \times 10^6$	$>10^6$	$>10^4$ (1D) $>10^6$ (2D)	$>8 \times 10^7$ (1D) $>10^9$ (2D)
Maximum global count rate	$>2 \times 10^6$ c.p.s.	$>7.5 \times 10^5$	$>10^5$ (1D) $>4 \times 10^4$ c.p.s. (2D)	$>8 \times 10^5$ (1D) $>1.6 \times 10^6$ c.p.s. (2D)
Maximum local count rate	n/a	n/a	$>10^4$ (1D) $>10^4$ c.p.s. mm^{-2} (2D)	$>9 \times 10^5$ c.p.s. mm^{-2} (1D, 2D)
Noise	∼0.3 c.p.s.	∼1 c.p.s.	∼1 c.p.s. (1D) $<5 \times 10^{-4}$ c.p.s. mm^{-2} (2D)	<0.01 c.p.s. (1D) $<5 \times 10^{-4}$ c.p.s. mm^{-2} (2D)
Energy resolution	∼3500 eV (∼45%)	∼1600 eV (∼20%)	∼1600 eV (∼20%)	∼1600 eV (∼20%)
Detection mode	Photon counting	Photon counting	Photon counting	Photon counting

	Semiconductor				
	Si(Li)	Strip	Pixel	CCD	CMOS
DQE	>98%	>98%	>98%	∼20–60%	∼75%
Dynamic range	$>10^6$	$>7 \times 10^6$ per strip	$>10^9$	$>5 \times 10^4$	$>1.6 \times 10^4$
Maximum global count rate	$>10^5$ c.p.s.	$>10^8$ c.p.s	$>10^7$ c.p.s. mm^{-2}	n/a	n/a
Maximum local count rate	n/a	$>7 \times 10^5$ c.p.s. per strip	$>10^4$ per pixel	n/a	n/a
Noise	∼0.1 c.p.s.	∼0.1 c.p.s. per strip	$\sim 2.5 \times 10^{-3}$ c.p.s. mm^{-2}	<0.1 c.p.s. per pixel	<0.05 c.p.s. per pixel
Energy resolution	∼200 eV (∼4%)	∼1600 eV (∼20%)†	>1000 eV (∼12.5%)	n/a‡	n/a
Detection mode	Photon counting	Photon counting	Photon counting	Integrating§	Integrating

† ∼380 eV/∼5%; Wiacek *et al.* (2015). ‡ >300 eV/>6% in photon-counting mode, see text. § Photon-counting mode possible, see text.

as the detector of choice. An important disadvantage these days is the limitation to 0D detection.

2.1.7.2.2. *Gas-ionization detectors*

The gas-ionization detectors in current use are proportional counters and can be of the 0D, 1D or 2D detection type. Common to all proportional counters is a gas-filled chamber permeated by a non-uniform electric field between positive and negative electrodes, held at a constant potential difference relative to each other. Typically the noble gases Ar or Xe are used as gas fill, mixed with a small amount of quenching gas such as CH_4 or CO_2 to limit discharges. When an X-ray photon travels through the gas-filled volume, it may be absorbed by a noble-gas atom, resulting in the ejection of an electron (photoelectric and Compton recoil). This electron, accelerated by the electric field towards the anode, will cause an avalanche by subsequent ionization along its path (gas amplification), generating an electric pulse which can be registered. The height of the generated pulse is proportional to the energy of the incoming X-ray photon and permits the use of pulse-height selection to achieve moderate energy resolution.

2.1.7.2.2.1. Wire-based proportional counters

In a point proportional detector (0D detection), the pulses generated are measured at one end of a wire (or a knife edge). Position-sensitive (1D and 2D detection) proportional detectors have the added capability of detecting the location of an X-ray photon absorption event. In a 1D proportional detector, pulses are detected at both ends of the wire. Thus the time difference between the measurements of a given pulse can be used to determine the location of the discharge. 2D proportional counters consist of three arrays of wires (multiwire proportional counter, MWPC; Sauli, 1977; Charpak *et al.*, 1968), where one array forming the anode plane is placed between two cathode arrays with their wires oriented parallel and orthogonal to the anode-plane wires, respectively.

Low count rates and low-to-moderate detector noise result in low-to-moderate dynamic ranges. Wire-based proportional counters are not competitive with micro-gap and semiconductor detectors, as can be seen in Table 2.1.6, and are therefore being driven out of the market.

2.1.7.2.2.2. Micro-gap detectors

The maximum count rates in 'classical' metal-wire-based proportional counters are severely limited by the long ion-drift times in the chamber (which typically have a cathode to anode spacing of ∼10 mm). This issue has been successfully addressed by so-called micro-gap technology using parallel-plate avalanche chambers with a readout electrode separated from a resistive anode. The key feature is the resistive anode, which allows a very small amplification gap (1–2 mm cathode to anode spacing) at an increased average electric field intensity, while preventing discharges (Durst *et al.*, 2003; Khazins *et al.*, 2004). As a result, micro-gap detectors can achieve count rates several orders of magnitude higher than classical proportional counters at higher position sensitivity. Micro-gap detectors of the 1D and 2D detection type are available. Moderate count rates and very small

noise levels result in very high dynamic ranges. Notably, in contrast to wire detectors, micro-gap detectors are not likely to be damaged by accidental exposure to a high-intensity direct beam, as a patterned anode plane is used rather than wires.

2.1.7.2.3. *Semiconductor detectors*

Semiconductor (or solid-state) detectors are solid-state ionization devices in which electron–hole pairs instead of electron–ion pairs are generated by incoming photons, and they are sensitive to the entire electromagnetic spectrum from visible light to X-rays. The energy required for production of an electron–hole pair is very low compared to the energy required for production of paired ions in a noble-gas-filled detector. As a consequence, a larger number of charge pairs with a smaller statistical variation are generated in semiconductor detectors, resulting in intrinsically higher energy-resolution capabilities. The efficiency of semiconductor detectors is very high due to the high absorption of the semiconductor materials, usually reaching 100%, but may decline at higher photon energies if the photons are not fully absorbed in the semiconductor *e.g.* because of insufficient thickness.

2.1.7.2.3.1. The Si(Li) detector

The Si(Li) detector sensor consists of a lithium-drifted silicon crystal which must be cooled to prevent lithium diffusion and to reduce dark noise. An important advantage of this detector is its excellent energy resolution of even better than 200 eV (4%) at 8 keV (Cu radiation), allowing very effective filtering of Kβ and fluorescence radiation and thus operation without a metal filter or a diffracted-beam monochromator. As Peltier cooling is sufficient, the Si(Li) detector type has found wide interest for applications benefitting from high energy resolution, unlike energy-dispersive detectors requiring operation under cryogenic conditions [*e.g.* Ge(Li)]. In particular, the Si(Li) detector significantly extends the application range of today's X-ray diffractometers by allowing energy-dispersive X-ray powder diffraction (EDXRD) as well as – to some extent – XRF (see Section 2.1.4.3).

An important disadvantage of Si(Li) detectors is their large dead time, which prohibits the handling of higher count rates. Moderate noise levels result in low-to-moderate dynamic ranges. An additional important disadvantage is the limitation to 0D detection.

2.1.7.2.3.2. Silicon micro-strip and silicon pixel detectors

Silicon micro-strip and silicon pixel detectors employ silicon sensors, which are one- or two-dimensional arrays of p–n diodes in the form of strips or pixels, respectively, individually connected to an array of readout channels. The development of this type of detector technology has obviously been driven by the idea of massive parallelism: each strip or pixel actually represents an individual detector. Accordingly, the silicon micro-strip and silicon pixel detectors are therefore of the 1D and 2D detection type, respectively.

Count rates recorded by silicon micro-strip and silicon pixel detectors are very high with very low noise levels, resulting in very large dynamic ranges. The energy resolution of most silicon micro-strip and silicon pixel detectors is of the order of 1600 eV (20%) at 8 keV (Cu radiation). Recently, a silicon micro-strip detector with an energy resolution of better than 380 eV at 8 keV has been introduced (Wiacek *et al.*, 2015). At such high energy resolution Cu Kβ is filtered out to below the detection limit while Mn, Fe and Co fluorescence is filtered completely, allowing this detector to be operated without a metal filter or a diffracted-beam monochromator for most applications.

2.1.7.2.3.3. CCD and CMOS detectors

Charge-coupled device (CCD) detectors are represented by one- or two-dimensional arrays of square or rectangular pixels consisting of metal–oxide–semiconductor (MOS) capacitors, and can detect X-ray photons directly or indirectly. The pixel size may be less than 10 µm. The majority of detectors use indirect detection, where the incoming X-ray photons are first converted to visible-light photons by a phosphor layer. CCD detectors employ the 'bucket brigade' readout method, in which charge is shifted one pixel at a time by phasing the bias on the gate electrodes that overlay each pixel until it reaches the output, resulting in relatively large readout times ranging from a few tenths of a second up to several seconds per frame. Cooling (Peltier-type) is required to reduce the dark-current noise representing the dominant noise source for long exposures. In some detector designs fibre-optic demagnification is used to increase the effective active detector area, resulting in an imaging area larger than the active area of the CCD chip at the cost of detector sensitivity and spatial resolution.

CCD detectors are usually operated as integrating detectors. As such, they have no dead time and therefore provide excellent linearity over a moderate dynamic range, but cannot have energy resolution. CCD detectors are the detectors of choice for single-crystal diffraction and imaging, but are not favourable for applications with weak diffraction signals, such as powder X-ray diffraction, owing to the relatively large dark-current noise.

CCD detectors may also function as counting detectors by making the exposure time sufficiently short. In single-event mode the energy of each photon can be determined, providing an energy resolution down to about 300 eV at 8 keV (Cu radiation) and allowing a spectrum at each pixel of the CCD array to be built up by a series of consecutive measurements. Such a detector can record energy-dispersive X-ray powder diffraction (EDXRD) as well as – to some extent – XRF (see Section 2.1.4.3); however, owing to the readout time, count rates are extremely low with high statistical noise.

Unlike the bucket-brigade readout of a CCD, the complementary metal–oxide–semiconductor (CMOS) active-pixel sensor (He *et al.*, 2011) uses a completely different architecture in which each pixel incorporates a readout preamplifier and is then read out through a bus, as in random-access memory (He *et al.*, 2011). Cooling is not required. CMOS detectors are immune to the blooming effect (in which a light source overloads the sensitivity of the sensor, causing the signal to bleed vertically into surrounding pixels forming vertical streaks). Additionally, they offer the very significant advantage of shutter-free operation, that is dead-time-free continuous scans which improve the efficiency of data collection and also improve data quality by eliminating shutter-timing jitter.

As a consequence of these characteristics, CMOS-detector active-pixel sensors are now replacing CCD chips in a number of high-end applications (*e.g.* professional digital photography and high-definition television), and have reached a level of performance where they are also starting to displace CCD chips in the most demanding scientific applications.

2.1.7.3. *Position sensitivity and associated scanning modes*

2.1.7.3.1. *Pixel size, spatial resolution and angular resolution*

Detectors of the line (1D) or area (2D) type have the important property of position sensitivity, which is characterized by the two parameters pixel size and spatial resolution.

The pixel size of a position-sensitive detector (PSD) can be represented either by the intrinsic size of the smallest addressable sensitive component of a detector (*e.g.* the actual size of the diodes), which can be binned to form larger pixels, or is set by the readout electronics (*e.g.* for wire-based detectors such as proportional counters). The spatial resolution is determined by the actual pixel size, the point-spread function (PSF) and parallax. The PSF represents the spread of a signal produced by a single photon over several pixels by mapping the probability density that a photon is recorded by a pixel in the vicinity of the point that the photon hit. Parallax will lead to an additional smearing if the photon travels at an angle to the detector normal. The final angular resolution of a detector system is given by the spatial detector resolution and the specimen-to-detector distance.

Point (0D) detectors do not provide position sensitivity, regardless of the actual size of the active window (representing a single pixel). Simply speaking, in analogy to PSDs, the spatial resolution of a point detector is determined by the goniometer step size representing the actual pixel size, and the size of the detector slit representing the PSF. As for PSDs, the angular resolution is given by the spatial resolution and the specimen-to-detector distance.

Detectors can be operated in fixed as well as in (2θ) scanning mode, where the step size is usually determined by the detector pixel size. Subsampling, that is scanning using an angular step size smaller than the angular pixel resolution, may be used to improve observed line profile shapes if the pixel resolution is too small. As a rule of thumb some 5–8 data points need be collected over the FWHM of a diffraction peak to allow for an appropriate description of the line-profile shape.

2.1.7.3.2. *Dimensionality*

Area detectors can be operated as line or point detectors. Electronic binning of the pixels into columns will form a line detector, while binning all pixels together will form a point detector, each associated with improvements of count rates and thus dynamic ranges. Alternatively, 1D or 0D 'regions of interest' can be defined electronically and/or by mounting suitable diffracted-beam-path X-ray optics. Area detectors – when operated as such – require point-focus operation.

Line detectors can be used as point detectors, which may be formed in several ways. One way is to only use one or more central pixels by either electronically switching off outer pixels and/or by mounting suitable X-ray optics. Another way is to turn the detector by 90° and to bin all pixels, leading to an improved count rate and thus dynamic range.

Obviously, when turning a line detector by 90°, it will function as an area detector if it is scanned over an angular range; the trace of the scan will form a cylindrical surface that is a two-dimensional diffraction image (He, 2009). This scan mode may be associated with a few advantages, in addition to lower costs. For example, the elimination of parallax and the possibility of using diffracted-beam-path optics improve the angular resolution in the 2θ direction and allow air scattering to be reduced.

2.1.7.3.3. *Size and shape*

PSDs are available in different sizes with flat (1D, 2D), curved (1D), cylindrical (2D) and spherical (2D) detection surfaces. Curved, cylindrical and spherical detectors are designed for focusing or parallel-beam geometries with a fixed specimen-to-detector distance, and cannot normally be used with the Bragg–Brentano geometry because of its 2θ-dependent focusing circle (Section 2.1.4.1). Flat detectors can be used at different specimen-to-detector distances, with either high angular resolution at a large distance or large angular coverage at a short distance. For large flat detectors, parallax errors must be addressed. Small flat detectors are perfectly suited for operation in Bragg–Brentano geometry but the angular coverage should not exceed about 10° 2θ (Section 2.1.4.1) to minimize defocusing, particularly at small 2θ angles.

References

Bartels, W. J. (1983). *Characterization of thin layers on perfect crystals with a multipurpose high resolution X-ray diffractometer*. *J. Vac. Sci. Technol. B*, **1**, 338–345.

Bilderback, D. H. (2003). *Review of capillary X-ray optics from the 2nd International Capillary Optics Meeting*. *X-ray Spectrom.* **32**, 195–207.

Bohlin, H. (1920). *Eine neue Anordnung für röntgenkristallographische Untersuchungen von Kristallpulver*. *Ann. Phys.* **366**, 421–439.

Bonse, U. & Hart, M. (1965). *Tailless X-ray single crystal reflection curves obtained by multiple reflection*. *Appl. Phys. Lett.* **7**, 238–240.

Bowen, D. K. & Tanner, B. K. (1998). *High Resolution X-ray Diffractometry and Topography*. London: Taylor & Francis.

Brentano, J. C. M. (1924). *Focussing method of crystal powder analysis by X-rays*. *Proc. Phys. Soc.* **37**, 184–193.

Charpak, G., Bouclier, R., Bressani, T., Favier, J. & Zupančič, Č. (1968). *The use of multiwire proportional counters to select and localize charged particles*. *Nucl. Instrum. Methods*, **62**, 262–268.

Clearfield, A., Reibenspiess, J. & Bhuvanesh, N. (2008). *Principles and Applications of Powder Diffraction*. New York: Wiley.

Debye, P. & Scherrer, P. (1916). *Interference of X-rays, employing amorphous substances*. *Phys. Z.* **17**, 277–283.

Durst, R. D., Diawara, Y., Khazins, D. M., Medved, S., Becker, B. L. & Thorson, T. A. (2003). *Novel, photon counting X-ray detectors*. *Powder Diffr.* **18**, 103–105.

EN 1330–11 (2007). *Non-Destructive Testing*. Part 11. *Terms used in X-ray Diffraction from Polycrystalline and Amorphous Materials*. Brussels: European Committee for Standardization (CEN).

Fankuchen, I. (1937). *A condensing monochromator for X-rays*. *Nature (London)*, **139**, 193–194.

Fewster, P. F. (2003). *X-ray Scattering from Semiconductors*. London: Imperial College Press.

Friedmann, H. (1945). *Geiger counter spectrometer for industrial research*. *Electronics*, **18**, 132–137.

Göbel, H. E. (1980). *The use and accuracy of continuously scanning position-sensitive detector data in X-ray powder diffraction*. *Adv. X-ray Anal.* **24**, 123–138.

Guinier, A. (1937). *Arrangement for obtaining intense diffraction diagrams of crystalline powders with monochromatic radiation*. *C. R. Acad. Sci. Paris*, **204**, 1115–1116.

Hanawalt, J. D., Rinn, H. W. & Frevel, L. K. (1938). *Chemical analysis by X-ray diffraction*. *Ind. Eng. Chem. Anal.* **10**, 457–512.

Hart, M. (1971). *Bragg-reflection X-ray optics*. *Rep. Prog. Phys.* **34**, 435–490.

He, B. B. (2009). *Two-Dimensional X-ray Diffraction*. New York: Wiley.

He, T., Durst, R. D., Becker, B. L., Kaercher, J. & Wachter, G. (2011). *A large area X-ray imager with online linearization and noise suppression*. *Proc. SPIE*, **8142**, 81421Q.

Hemberg, O. E., Otendal, M. & Hertz, H. M. (2003). *Liquid-metal-jet anode electron-impact X-ray source*. *Appl. Phys. Lett.* **83**, 1483–1485.

Hull, A. W. (1917). *A new method of X-ray crystal analysis*. *Phys. Rev.* **10**, 661–696.

Hull, A. W. (1919). *A new method of chemical analysis*. *J. Am. Chem. Soc.* **41**, 1168–1175.

International Tables for Crystallography (2004). Volume C, 3rd ed., edited by E. Prince. Dordrecht: Kluwer Academic Publishers.